

Isospin transport phenomena in heavy ion collisions at Fermi energies: An overview on the most recent results from the first INDRA-FAZIA experiment

C. CIAMPI⁽¹⁾, S. PIANTELLI⁽²⁾, G. CASINI⁽²⁾, J. D. FRANKLAND⁽¹⁾,
L. BALDESI⁽²⁾⁽³⁾, S. BARLINI⁽²⁾⁽³⁾, B. BORDERIE⁽⁴⁾, R. BOUGAULT⁽⁵⁾,
A. CAMAIANI⁽²⁾⁽³⁾, A. CHBIHI⁽¹⁾, D. DELL'AQUILA⁽⁶⁾⁽⁷⁾, J. A. DUEÑAS⁽⁸⁾,
Q. FABLE⁽⁹⁾, C. FROSIN⁽²⁾⁽³⁾, T. GÉNARD⁽¹⁾, F. GRAMEGNA⁽¹⁰⁾, D. GRUYER⁽⁵⁾,
M. HENRI⁽¹⁾, B. HONG⁽¹¹⁾⁽¹²⁾, S. KIM⁽¹³⁾, A. KORDYASZ⁽¹⁴⁾, T. KOZIK⁽¹⁵⁾,
M. J. KWEON⁽¹⁶⁾, J. LEMARIÉ⁽¹⁾, N. LE NEINDRE⁽⁵⁾, I. LOMBARDO⁽¹⁷⁾⁽¹⁸⁾,
O. LOPEZ⁽⁵⁾, T. MARCHI⁽¹⁰⁾, K. MAZUREK⁽¹⁹⁾, S. H. NAM⁽¹¹⁾⁽¹²⁾, J. PARK⁽¹¹⁾⁽¹²⁾,
J. H. PARK⁽¹¹⁾, M. PÂRLOG⁽⁵⁾⁽²⁰⁾, G. PASQUALI⁽²⁾⁽³⁾, G. POGGI⁽²⁾⁽³⁾,
A. REBILLARD-SOULIÉ⁽⁵⁾, A. A. STEFANINI⁽²⁾⁽³⁾, S. UPADHYAYA⁽¹⁵⁾, S. VALDRÉ⁽²⁾,
G. VERDE⁽¹⁷⁾⁽⁹⁾, E. VIENT⁽⁵⁾ and M. VIGILANTE⁽⁶⁾⁽⁷⁾

⁽¹⁾ *Grand Accélérateur National d'Ions Lourds (GANIL), CEA/DRF-CNRS/IN2P3
Boulevard Henri Becquerel 14076 Caen, France*

⁽²⁾ *INFN, Sezione di Firenze - 50019 Sesto Fiorentino, Italy*

⁽³⁾ *Dipartimento di Fisica e Astronomia, Università di Firenze - 50019
Sesto Fiorentino, Italy*

⁽⁴⁾ *Université Paris-Saclay, CNRS/IN2P3, IJCLab - 91405 Orsay, France*

⁽⁵⁾ *Université de Caen Normandie, ENSICAEN, CNRS/IN2P3, LPC Caen UMR6534,
F-14000 Caen, France*

⁽⁶⁾ *INFN, Sezione di Napoli - 80126 Napoli, Italy*

⁽⁷⁾ *Dipartimento di Fisica, Università di Napoli - 80126 Napoli, Italy*

⁽⁸⁾ *Departamento de Ingeniería Eléctrica y Centro de Estudios Avanzados en Física,
Matemáticas y Computación, Universidad de Huelva - 21007 Huelva, Spain*

⁽⁹⁾ *Laboratoire des 2 Infinis, Toulouse (L2IT-IN2P3), Université de Toulouse, CNRS, UPS
F-31062 Toulouse Cedex 9 France*

⁽¹⁰⁾ *INFN, Laboratori Nazionali di Legnaro - 35020 Legnaro, Italy*

⁽¹¹⁾ *Center for Extreme Nuclear Matters, Korea University - Seoul 02841, Republic of Korea*

⁽¹²⁾ *Department of Physics, Korea University - Seoul 02841, Republic of Korea*

⁽¹³⁾ *Center for Exotic Nuclear Studies, IBS - Daejeon 34126, Republic of Korea*

⁽¹⁴⁾ *Heavy Ion Laboratory, University of Warsaw - 02-093 Warszawa, Poland*

⁽¹⁵⁾ *Marian Smoluchowski Institute of Physics Jagiellonian University
30-348 Krakow, Poland*

⁽¹⁶⁾ *Department of Physics, Inha University - Incheon 22212, Republic of Korea*

⁽¹⁷⁾ *INFN, Sezione di Catania - 95123 Catania, Italy*

⁽¹⁸⁾ *Dipartimento di Fisica e Astronomia, Università di Catania - via S. Sofia 64,
95123 Catania, Italy*

⁽¹⁹⁾ *Institute of Nuclear Physics Polish Academy of Sciences - PL-31342 Krakow, Poland*

⁽²⁰⁾ *“Horia Hulubei” National Institute for R&D in Physics and Nuclear Engineering
(IFIN-HH) - P. O. Box MG-6, Bucharest Magurele, Romania*

received 26 November 2024

Summary. — The coupled INDRA-FAZIA apparatus is operating in GANIL since 2019, when its first experiment has been carried out. In this experiment, the four reactions $^{58,64}\text{Ni}+^{58,64}\text{Ni}$ at 32 and 52 MeV/nucleon have been investigated in order to highlight the isospin transport effects on the neutron content of light and heavy fragments, particularly those belonging to the QP phase space which are collected by FAZIA. Here, we give an overview of the characteristics and performances of the coupled apparatus, as well as a summary of the most recent results and observations on this first rich dataset.

1. – Introduction

Heavy ion collisions allow to access transient nuclear environments where a wide variety of phenomena can take place, depending on conditions such as the bombarding energy and the reaction centrality [1]. The observation of the behavior of the interacting nuclei allows to collect information on multiple aspects and properties of nuclear forces.

Among the plethora of mechanisms that characterize the collision dynamics at intermediate energies, a widely studied one is isospin transport [2]. The interest in such phenomena stems from the fact that in the framework of the nuclear Equation of State (nEoS) they can be described as governed by the nEoS isovector term, called symmetry energy E_{sym} , expressing its dependence on isospin asymmetry. Two main contributions to isospin transport are generally distinguished: the isospin drift, leading to a net neutron flux towards lower density areas, and the isospin diffusion, that tends to re-equilibrate any isospin imbalance in the system. An experimental observation commonly ascribed to the former contribution is the neutron enrichment of midvelocity emissions possibly originating from a diluted neck area connecting projectile and target during non-central collisions. On the other hand, the latter contribution is considered responsible of the isospin equilibration observed on the quasiprojectile and quasitarget emerging from asymmetric reactions.

The experimental investigation of isospin transport phenomena requires detection setups capable of identifying the fragments produced in the reaction both by charge and mass, ideally over the widest possible range in energy and atomic number. Another desirable feature of the experimental apparatus is the ability to provide a good global event reconstruction, which can be achieved thanks to a large angular coverage with high granularity. In this context, the coupling of the INDRA and FAZIA setups was planned in order to collect the most comprehensive information on an intermediate-energy reaction by exploiting the best characteristics of the two apparatuses [3], as explained in the following.

2. – The INDRA-FAZIA apparatus

INDRA and FAZIA are two detection arrays both optimized to detect and identify charged products of heavy ion collisions at intermediate energies, but they nevertheless present some complementary features.

FAZIA [4, 5] is a new generation setup able to provide an optimal ion identification in the Fermi energy domain. The basic module is the block, *i.e.*, a 4×4 matrix of Si1 ($300 \mu\text{m}$) - Si2 ($500 \mu\text{m}$) - CsI (10 cm) telescopes. Each block incorporates the electronics required for the readout of all of its telescopes, including FPGAs carrying out the digital treatment of the signals and extracting from them most of the relevant quantities in real time. With this three-stage telescope configuration different identification techniques can be applied depending on the stopping layer for each particle. Isotopic discrimination can be achieved up to $Z \sim 25$ with the $\Delta E-E$ method, and up to $Z \sim 22$ with pulse shape analysis in the first silicon detector. Pulse shape analysis is also applied to CsI signals for the identification of the most energetic light particles produced. A recent example of the identification performance of FAZIA can be visualized in the experimental nuclear chart shown in fig. 1 (right). The performance in terms of ion identification of FAZIA is crucial to access the isotopic characteristics of the heaviest fragments, such as the QP remnants produced in more peripheral collisions: for this reason, in the coupled apparatus, the twelve FAZIA blocks currently available are arranged in a wall configuration (shown in fig. 1 (left)) and placed at forward polar angles to identify the fragments belonging to the QP phase space, but the angular coverage is limited to $\theta \lesssim 14^\circ$ (depending on the distance from target).

The INDRA array was designed for the identification of charged products in the same energy regime. INDRA [6] is characterized by a large solid angle coverage with high granularity, allowing for a good reconstruction of events up to high multiplicities. INDRA detection modules are arranged in rings with cylindrical symmetry with respect to the beam axis. Each module is a multi-stage identification telescope, with different configurations depending on the ring. Charge discrimination can be achieved up to uranium, and mass discrimination up to $Z \sim 4-5$. Recently, the INDRA electronics for data acquisition and power supply has been fully replaced [7]: thanks to this major upgrade, the identification performance has sensibly improved, allowing now for mass discrimination up to $Z \sim 10$. In the actual coupled configuration, the polar angles for $\theta > 14^\circ$ are covered by 12 INDRA rings (out of the 17 original rings), which alone provide 80% of the 4π solid angle coverage.

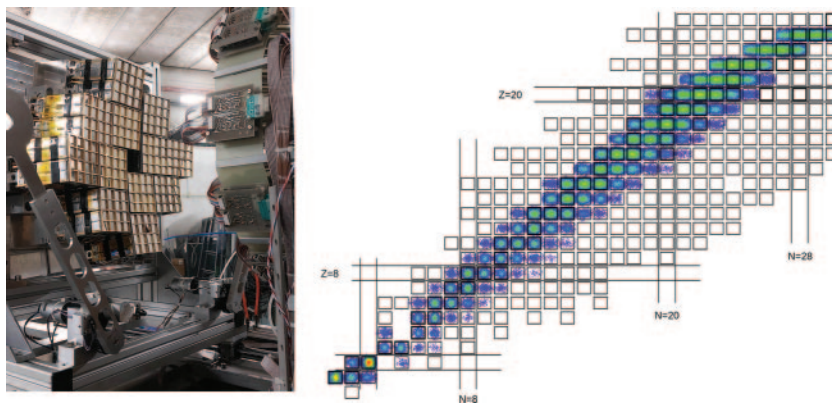


Fig. 1. – Left: photo of the 12 FAZIA blocks presently mounted in the D5 experimental hall in GANIL. Right: experimental nuclide chart obtained during the first INDRA-FAZIA experiment by applying the $\Delta E-E$ method on a typical Si1-Si2 FAZIA telescope.

3. – Recent results on isospin transport

The first INDRA-FAZIA experiment has been carried out in 2019, right after completing the coupling of the two apparatuses. In this experiment, the four reactions $^{58,64}\text{Ni}+^{58,64}\text{Ni}$ at 32 and 52 MeV/nucleon have been studied: the aim was to compare the products of the two asymmetric reactions with those of both the neutron rich and neutron deficient symmetric systems, in order to highlight the differences introduced in the output channel by the action of isospin diffusion.

3.1. Comparison between different bombarding energies. – We first focus on the outcome of semiperipheral and peripheral collisions, for which a binary channel is generally observed, with the production of the remnants of the QP and the quasitarget (QT) together with light emissions. We select the QP evaporation channel by requiring a single heavy fragment ($Z \geq 15$) in the forward hemisphere in the center-of-mass (CM) reference frame. We have verified that this cut selects events in which the only heaviest fragment has charge and velocity characteristics compatible with those of a QP remnant [8].

In order to follow the evolution of the isospin content of such heavy fragment with the reaction centrality, we select as centrality related observable the reduced momentum of the QP remnant $p_{red} = (p_z^{QP}/p_{beam})_{CM}$, p_z^{QP} being the QP remnant momentum component along the beam axis and p_{beam} the original projectile momentum. Its correlation with the reduced impact parameter $b_{red} = b/b_{grazing}$ has been tested with AMD+GEMINI++ simulations [9,10], resulting suitable for semiperipheral-to-peripheral collisions, almost independent of the system and only slightly dependent on the bombarding energy [8,11].

Finally, thanks to the isotopic discrimination provided by FAZIA, we can study the evolution of the $\langle N/Z \rangle$ of the QP remnant as a function of our centrality observable p_{red} . The result for the four reactions at 32 MeV/nucleon is shown in fig. 2 (left). A clear evidence of the dynamical effect of isospin diffusion is found in the increasing gap that develops for increasing centrality between the $\langle N/Z \rangle$ results for the asymmetric and symmetric reactions sharing the same projectile, that makes the results of the two asymmetric reactions tend towards each other. Similar observations can be done for the reactions at 52 MeV/nucleon [8]. The isospin equilibration in the asymmetric

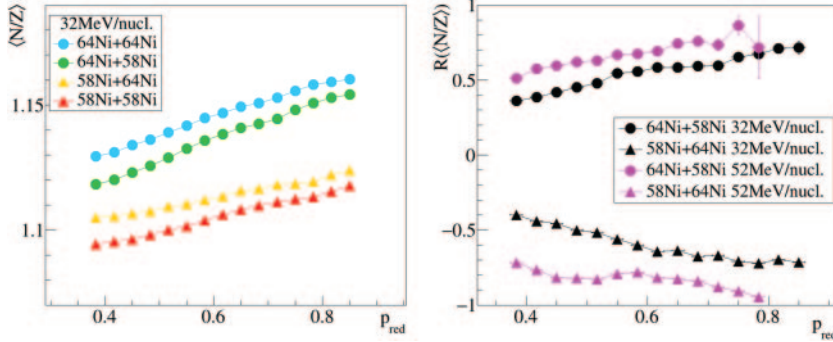


Fig. 2. – Left: experimental $\langle N/Z \rangle$ of the QP remnant in the evaporation channel as a function of p_{red} for the four reactions at 32 MeV/nucleon. Right: comparison between the experimental isospin transport ratio obtained with the $\langle N/Z \rangle$ of the QP remnant in the evaporation channel as a function of p_{red} , for the reactions at 32 and 52 MeV/nucleon.

systems can be better visualized by calculating the isospin transport ratio [12], defined as $R(X_i) = \frac{2X_i - X_{6464} - X_{5858}}{X_{6464} - X_{5858}}$ where i represents the two asymmetric systems and X an isospin sensitive observable such as the $\langle N/Z \rangle$ of the QP remnant in our case. By using the two symmetric reactions as references for normalization, the isospin transport ratio largely reduces the impact of the effects acting similarly on the four systems, including those associated to the experimental limitations or to the statistical de-excitation [13,14]. Figure 2 (right) shows the experimental isospin transport ratio $R(\langle N/Z \rangle)$ vs. p_{red} obtained for the asymmetric systems at the two beam energies. The evolution towards equilibration for increasing centrality is clear in both cases, with the two branches tending towards the same value for decreasing p_{red} . Moreover, by comparing the results for 32 and 52 MeV/nucleon, we note that a higher degree of isospin equilibration is achieved for the lower beam energy, as could be expected, *e.g.*, from the longer interaction timescale in that case. This different behavior remains clearly visible also after taking into account the small difference between the p_{red} vs. b_{red} correlations predicted by AMD+GEMINI++, and it has been coherently found also by employing a different observable, associated to the light emissions from the QP, as isospin probe to compute the isospin transport ratio [8].

3.2. Comparison between different reaction channels. – The granularity provided by FAZIA in the forward angle also allows us to investigate the output channel associated with the QP breakup or dynamical fission [15]. In fact, both forward-emitted QP fission fragments can be generally distinguished and mass-identified [11,16]. To select this reaction channel, we consider the events with a total multiplicity of heavy ($Z \geq 5$) fragments equal to 2. The events compatible with a QP breakup process are selected by applying further conditions on the relative angle and relative velocity of the two breakup fragment candidates [17]. The fissioning QP (Z_{rec}, A_{rec}) is thus “reconstructed” as the sum of the two daughter nuclei, with a velocity equal to that of their CM.

An isospin analysis similar to that performed on the QP remnant in the evaporation channel can also be applied to the reconstructed QP in the breakup channel. As for the binary channel, also here we select the breakup events where the reconstructed QP is forward emitted in the CM reference frame, with $Z_{rec} \geq 15$. The evolution of the $\langle N/Z \rangle$ of the reconstructed QP with centrality shows global features similar to those observed

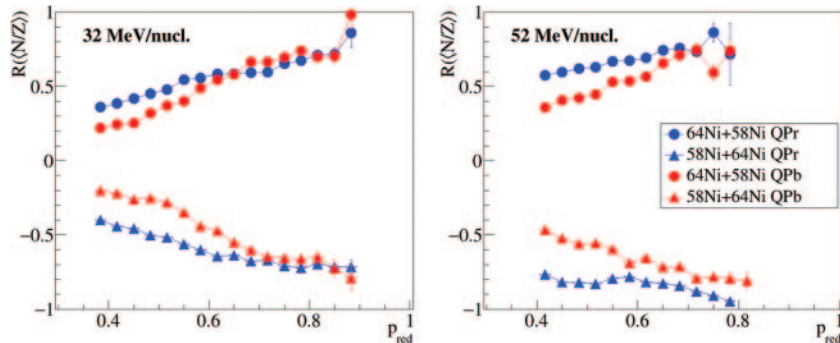


Fig. 3. – Experimental isospin transport ratio obtained with the $\langle N/Z \rangle$ of the QP remnant in the evaporation channel and of the reconstructed QP in the breakup channel, reported as a function of p_{red} , for the reactions at 32 (left) and 52 MeV/nucleon (right).

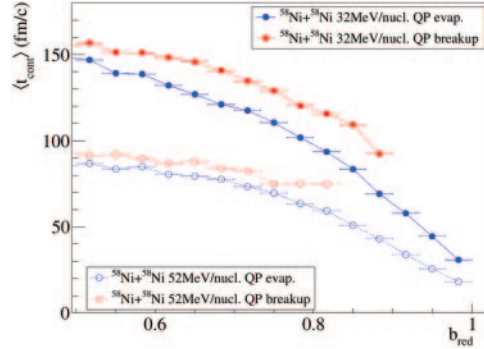


Fig. 4. – Average contact time extracted from AMD+GEMINI++ simulations for $^{58}\text{Ni}+^{58}\text{Ni}$ at the two beam energies, reported as a function of centrality.

for the QP remnant in the evaporation channel [17], with a clear trend towards isospin equilibration for less peripheral collisions, that we can again highlight by employing the isospin transport ratio. Figure 3 shows the comparison between the experimental results for the evolution with p_{red} of the isospin transport ratio computed from the $\langle N/Z \rangle$ of the reconstructed QP in the breakup channel and that of the QP remnant in the evaporation channel at the two beam energies: here, we have been able to observe an unexpected stronger tendency towards equilibration for the breakup channel with respect to the binary one. To possibly explain this experimental observation, we proposed an interpretation linking the QP dynamical fission events to longer projectile-target contact times during the interaction phase. These extended contact times allow for greater equilibration and induce a stronger deformation of the dinuclear system, finally resulting in a QP (or QT) breakup.

A similar observation regarding the differing degrees of equilibration in the two selected channels is found in the AMD+GEMINI++ simulations [9, 10] of the same Ni-Ni systems. We therefore extracted the contact time information from the AMD calculations to test our hypothesis [17]. The results for $^{58}\text{Ni}+^{58}\text{Ni}$ at the two beam energies are shown in fig. 4, where the average contact time is reported as a function of b_{red} with different colors associated with the two reaction channels. We note that $\langle t_{cont} \rangle$ evolves as expected with centrality and scales correctly with the beam energy, in support of the reliability of the extracted times. A systematic $\langle t_{cont} \rangle$ difference is found between the two selected outputs in the simulation, with breakup events associated to averagely longer interactions: according to the model, our hypothesis could at least partly explain the observed phenomenon. Similar results are found for the other systems [17].

4. – Conclusion and perspectives

In this contribution, we have presented the most recent results from the INDRA-FAZIA apparatus, focusing on its first experiment, which was devoted to the study of isospin transport in intermediate-energy collisions. We have mostly focused on isospin diffusion in semiperipheral to peripheral collisions, setting up an exclusive analysis with well-defined output channels. In the more populated binary exit channels, we have been able to highlight the different evolution towards equilibration associated with different bombarding energies. Moreover, at both beam energies, an unexpectedly different degree

of isospin equilibration has been observed between the QP evaporation and the QP breakup output channels, that we have been able to link with different average interaction timescales indirectly selected in the two cases.

Further analyses are being conducted on this rich first INDRA-FAZIA dataset: we are currently testing the model independent impact parameter reconstruction method proposed in ref. [18] in a less exclusive analysis to provide a more general result on the behavior of isospin diffusion as a function of the impact parameter, easily comparable with any simulation. Some very promising preliminary results have been obtained, and a paper on a first comparison with BUU@VECC-McGill predictions [14] is in preparation.

REFERENCES

- [1] COLONNA M., *Prog. Part. Nucl. Phys.*, **113** (2020) 103775.
- [2] BARAN V. *et al.*, *Phys. Rev. C*, **72** (2005) 064620.
- [3] CASINI G. and LE NEINDRE N., *Nucl. Phys. News*, **32** (2022) 24.
- [4] BOUGAULT R. *et al.*, *Eur. Phys. J. A*, **50** (2014) 47.
- [5] VALDRÉ S. *et al.*, *Nucl. Instrum. Methods Phys. Res. A*, **930** (2019) 27.
- [6] POUTHAS J. *et al.*, *Nucl. Instrum. Methods Phys. Res. A*, **357** (1995) 418; **369** (1996) 222.
- [7] FRANKLAND J. D. *et al.*, *Nuovo Cimento C*, **45** (2022) 43.
- [8] CIAMPI C. *et al.*, *Phys. Rev. C*, **106** (2022) 024603.
- [9] ONO A. *et al.*, *Prog. Theor. Phys.*, **87** (1992) 1185.
- [10] CHARITY R. J., *Phys. Rev. C*, **82** (2010) 014610.
- [11] CAMAIANI A. *et al.*, *Phys. Rev. C*, **103** (2021) 014605.
- [12] RAMI F. *et al.*, *Phys. Rev. Lett.*, **84** (2000) 1120.
- [13] CAMAIANI A. *et al.*, *Phys. Rev. C*, **102** (2020) 044607.
- [14] MALLIK S. *et al.*, *J. Phys. G: Nucl. Part. Phys.*, **49** (2022) 015102.
- [15] STEFANINI A. A. *et al.*, *Z. Phys. A*, **351** (1995) 167.
- [16] PIANTELLI S. *et al.*, *Phys. Rev. C*, **101** (2020) 034613.
- [17] CIAMPI C. *et al.*, *Phys. Rev. C*, **108** (2023) 054611.
- [18] FRANKLAND J. D. *et al.*, *Phys. Rev. C*, **104** (2021) 034609.